Обзор июля 2016 года

От Сильченко О.К.

Astro-ph: 1607.05726

An Improved Distance and Mass Estimate for Sgr A* from a Multistar Orbit Analysis

A. Boehle[1], A. M. Ghez[1], R. Schödel[2], L. Meyer[1], S. Yelda[1], S. Albers[1], G. D. Martinez[1], E. E. Becklin[1], T. Do[1], J. R. Lu[3], K. Matthews[4], M. R. Morris[1], B. Sitarski[1], G. Witzel[1]

aboehle@astro.ucla.edu

Теперь у 2х звезд замкнули орбиты!

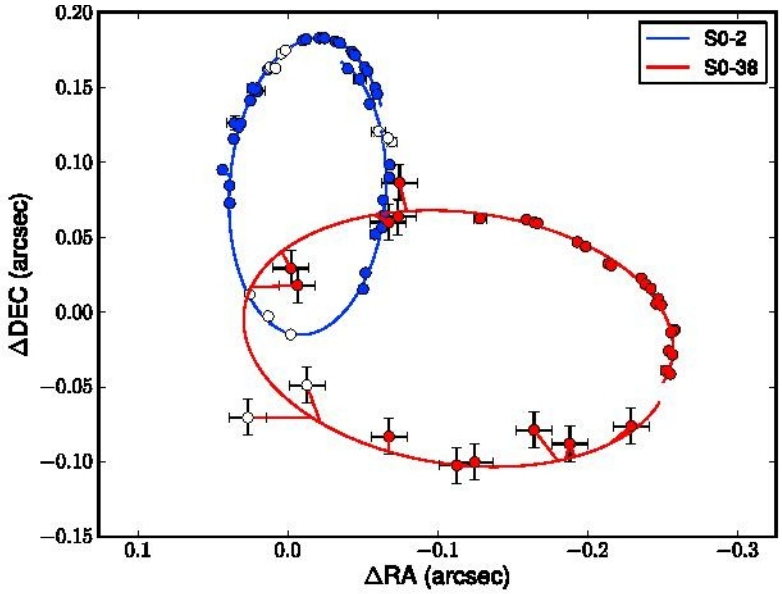

Fig. 5.— The best-fit orbit for S0-2 (blue line) and for S0-38 (red line) on the plane of the sky. These model orbit lines show the positions of these stars from 1995 to 2014. Both stars orbit clockwise on the plane of the sky. Closed circles indicate astrometric detections that were used in the orbital fits. Open circles indicate points that were not used in the fits because these astrometric detections are biased due to the proximity of other known sources on the plane of the sky. For S0-38, this consists of the two epochs

Уточнили параметры черной дыры вдвое!

Table 4. Best-Fit Black Hole and Orbital Parameters as Derived From the Fit of S0-2 alone, S0-38 alone, and the Simultaneous Fit of S0-2 and S0-38

Model Parameter (units)	Best-Fit Parameter Values from Orbital Fits[a]		
	S0-2 only	S0-38 only	S0-2 and S0-38
Black Hole Properties:			
Distance (kpc)	$8.02 \pm 0.36 \pm 0.04$	$[6.5, 9.5]$[b]	$7.86 \pm 0.14 \pm 0.04$
Mass ($10^6 M_\odot$)	$4.12 \pm 0.31 \pm 0.04$	$[2.5, 5.5]$[b]	$4.02 \pm 0.16 \pm 0.04$
X Position of Sgr A* (mas)	$2.52 \pm 0.56 \pm 1.90$	$-5.25 \pm 9.41 \pm 1.90$	$2.74 \pm 0.50 \pm 1.90$
Y Position of Sgr A* (mas)	$-4.37 \pm 1.34 \pm 1.23$	$-6.85 \pm 5.00 \pm 1.23$	$-5.06 \pm 0.60 \pm 1.23$
X Velocity (mas/yr)	$-0.02 \pm 0.03 \pm 0.13$	$-0.40 \pm 0.70 \pm 0.13$	$-0.04 \pm 0.03 \pm 0.13$
Y Velocity (mas/yr)	$0.55 \pm 0.07 \pm 0.22$	$-0.48 \pm 0.43 \pm 0.22$	$0.51 \pm 0.06 \pm 0.22$
Z Velocity (km/sec)	$-15 \pm 10 \pm 4$	$[-80, 40]$[b]	$-15.48 \pm 8.36 \pm 4.28$

Хи-квадрат…

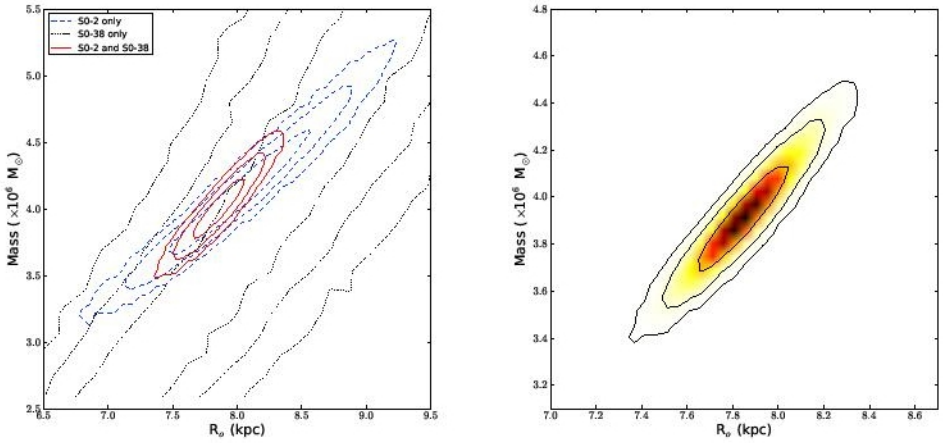

Fig. 10.— *Left*: 2D joint probability distribution with 1-, 2-, and 3-sigma contours of M_{bh} and R_o as derived by the orbital fit of S0-2 alone (blue dashed lines), S0-38 alone (black dotted line), and a simultaneous fit of S0-2 and S0-38, with the new speckle holography detections of S0-38 included (red solid lines). The

Astro-ph: 1607.06466

The supermassive black hole and double nucleus of the core elliptical NGC 5419⋆

Ximena Mazzalay,[1]† Jens Thomas,[1,2] Roberto P. Saglia,[1,2] Gary A. Wegner,[3] Ralf Bender,[1,2] Peter Erwin,[1] Maximilian H. Fabricius,[1,2,4] Stephanie P. Rusli[1,2]
[1]*Max-Planck-Institut für extraterrestrische Physik, Postfach 1312, 85741 Garching, Germany*
[2]*Universitätssternwarte, Scheinerstrasse 1, 81679 München, Germany*
[3]*Department of Physics and Astronomy, Dartmouth College, 6127 Wilder Laboratory, Hanover, NH 03755, USA*
[4]*Subaru Telescope, 650 North Aohoku Place, Hilo, HI 96720*

Почувствуйте разницу…(

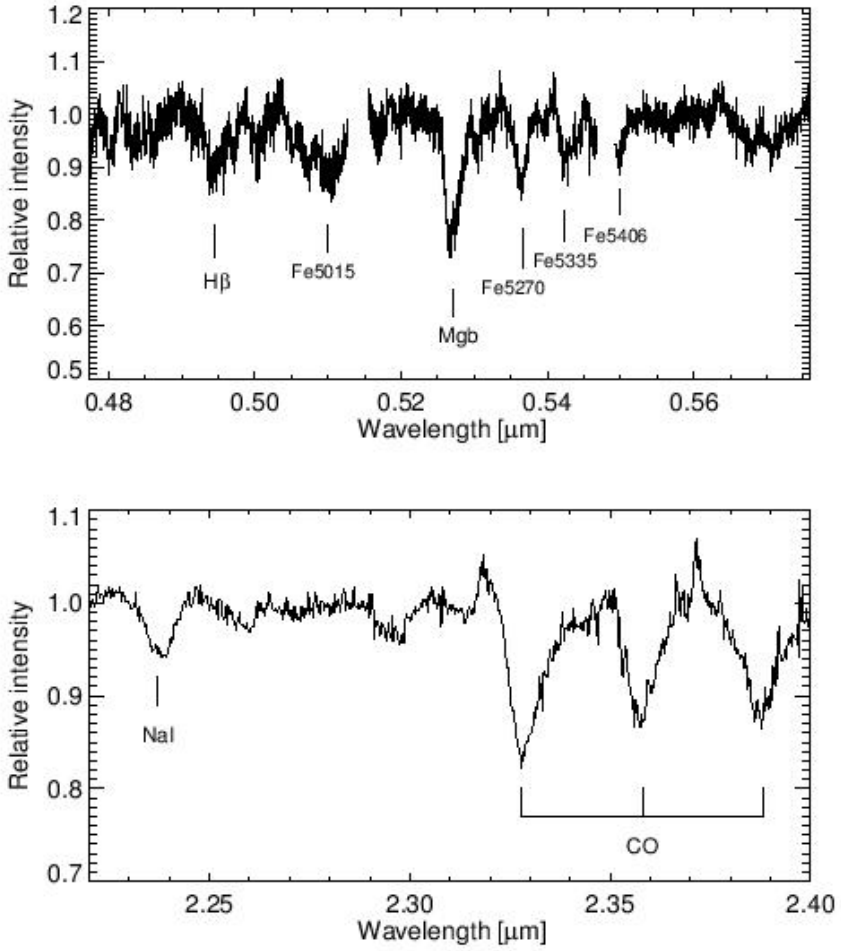

Figure 1. Optical (SALT, upper panel) and NIR (SINFONI, lower panel) continuum-normalized spectrum of NGC 5419, in the

Два ядра NGC 5419

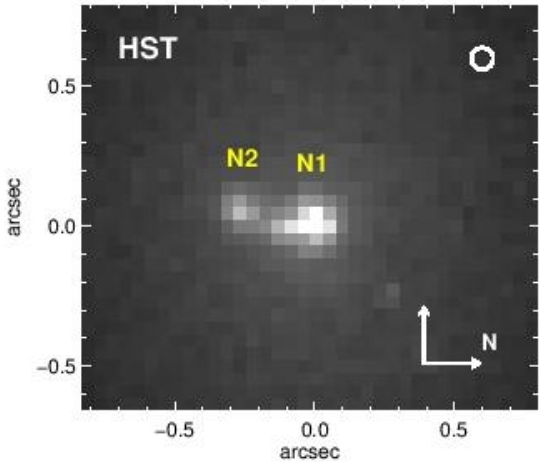

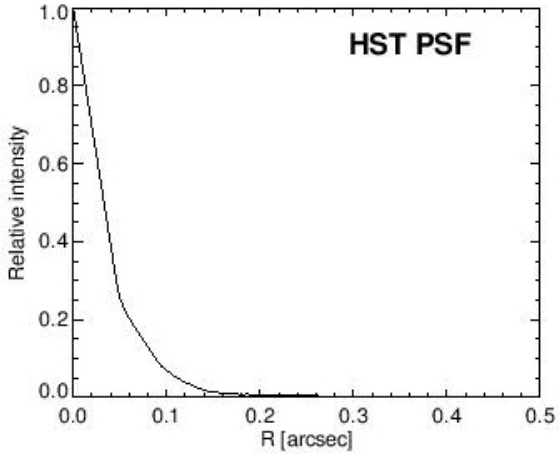

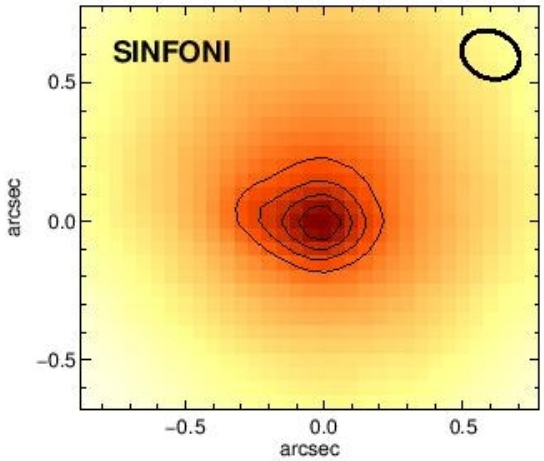

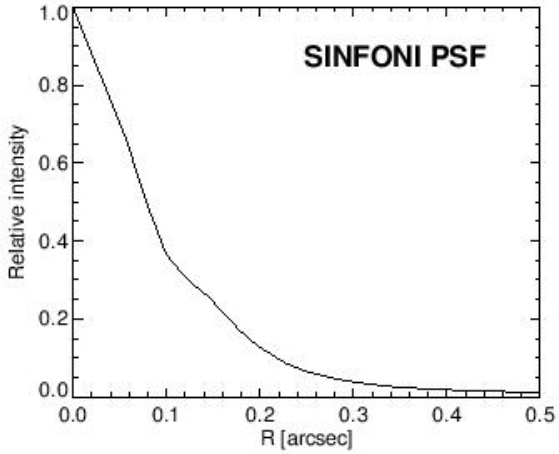

Противовращающийся центр и плоский максимум дисперсии скоростей

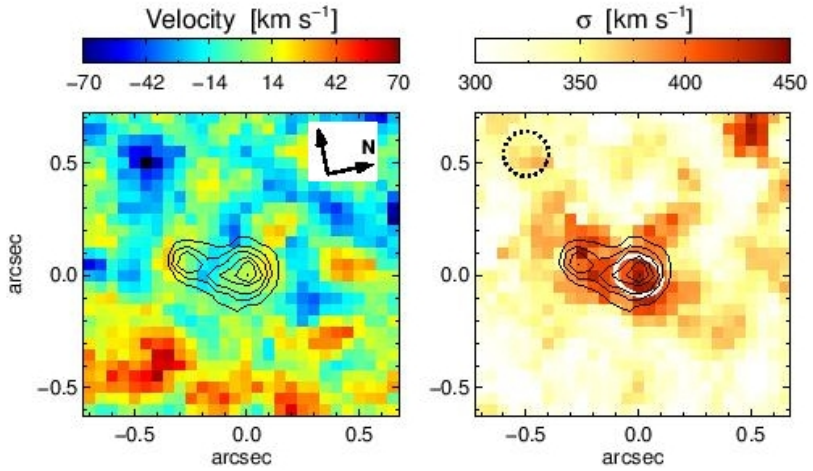

Figure 6. Velocity and velocity dispersion maps of the inner region of NGC 5419 derived from the SINFONI data. North is right and east is up. Overplotted are the isophotes of the *HST* image (see Fig. 2). The dashed circle and white ellipse in the right panel indicate the binning size and the Gaussian FWHM of the SINFONI PSF, respectively.

1993; Stiavelli et al. 1997), much bluer than the value of 1.68 we obtained for N2 (Section 3.2).

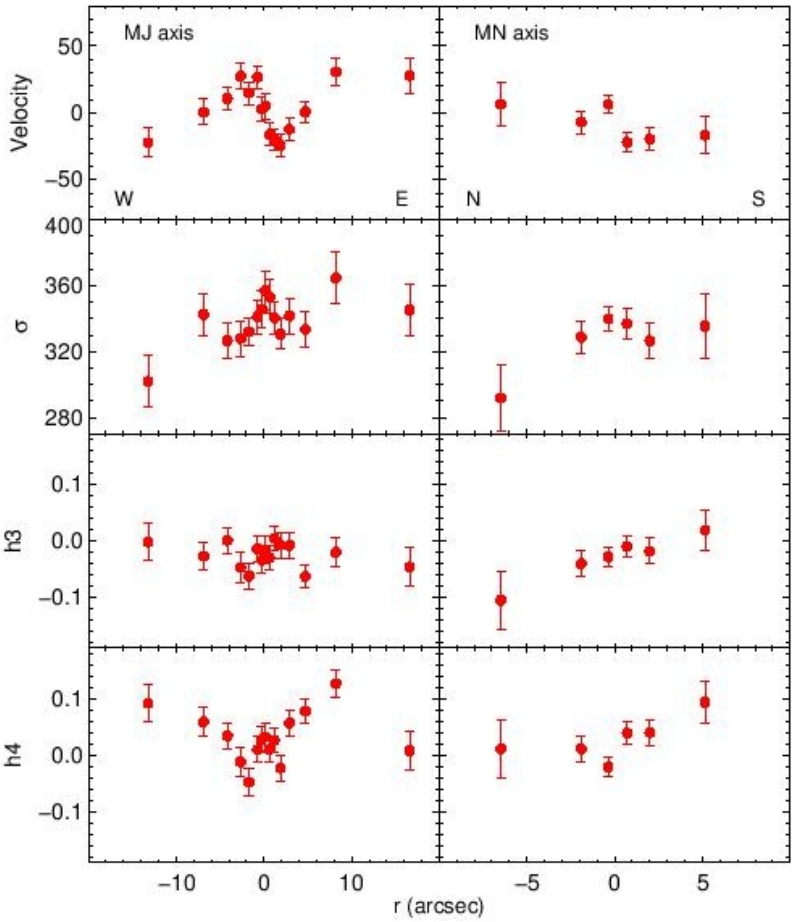

Черные дыры – в сумме 7 млрд солнечных масс

Astro-ph: 1607.07595

Exponential Disks from Stellar Scattering: III. Stochastic Models

Bruce G. Elmegreen[1], Curtis Struck[2]

Astro-ph: 1607.07595

1. Introduction

The exponential shape for the radial profiles of galaxy disks (de Vaucouleurs 1959) has never been explained at a fundamental level. The initial mass and angular momentum distribution in the gaseous halo plays a role early-on (Eggen et al. 1962; Mestel 1963; Fall & Efstathiou 1980), as they lead to a nearly exponential shape during collapse if angular momentum is conserved (Freeman 1970). Numerical simulations confirm this result even with some redistribution of angular momentum (e.g., Dalcanton et al. 1997; Governato et al. 2007; Foyle et al. 2008; Sánchez-Blázquez 2009; Cooper 2013; Aumer & White 2013; Aumer et al. 2013; Stinson et al. 2013; Martig 2014; Herpich et al. 2015; Minchev et al. 2015; Rathaus et al. 2016). Initial conditions also seem involved for the far-outer gas disks of HI-rich galaxies, which have exponential profiles with a universal scale length when normalized to the radius where the HI surface density is 1 $M_\odot$ pc^{-2} (Wang et al. 2014). Bigiel & Blitz (2012) found a universal exponential gas profile when normalized to R_{25}, the radius at 25 magnitudes per square arcsec in the V band.

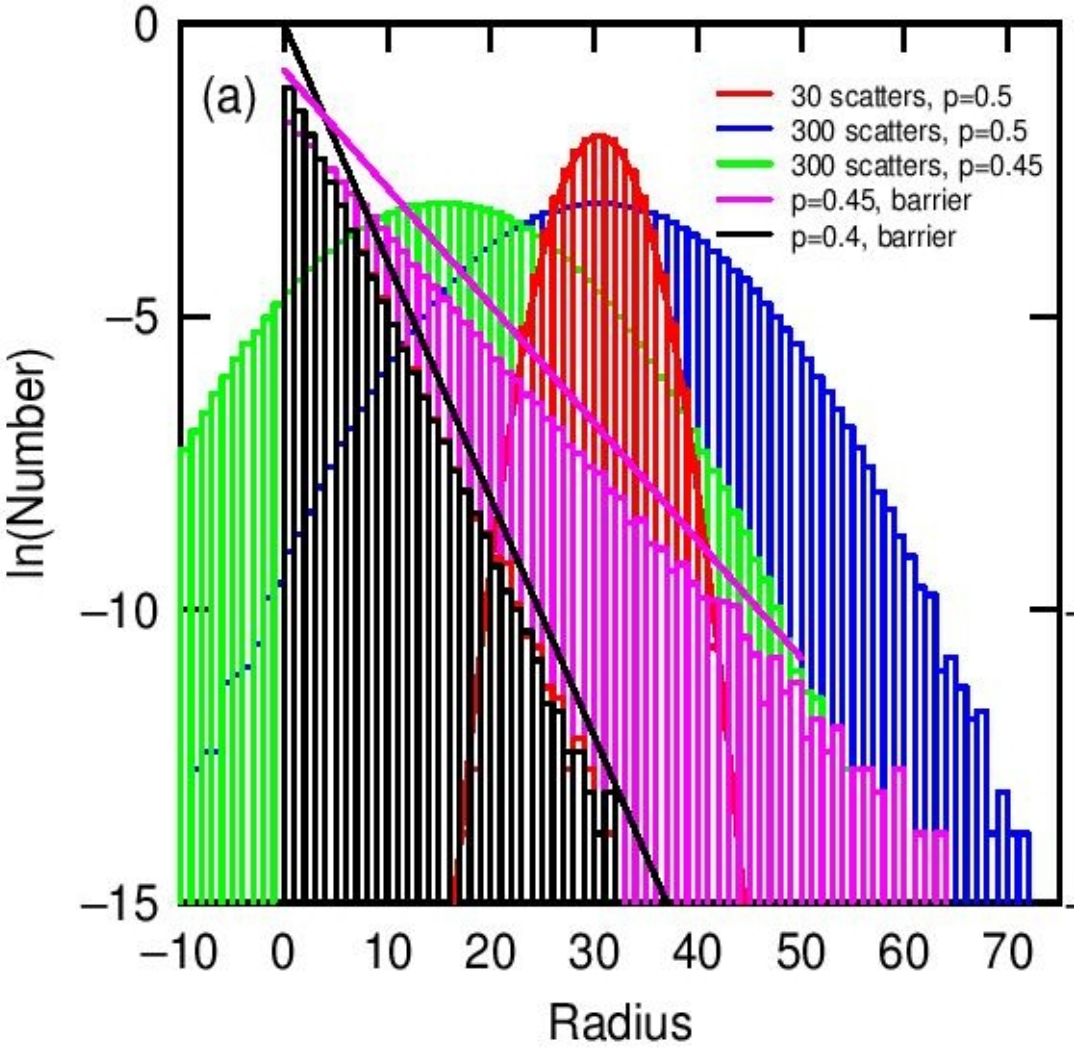
(a)
30 scatters, p=0.5
300 scatters, p=0.5
300 scatters, p=0.45
p=0.45, barrier
p=0.4, barrier
ln(Number)
0
−5
−10
−15
−10
0
10
20
30
40
50
60
70
Radius

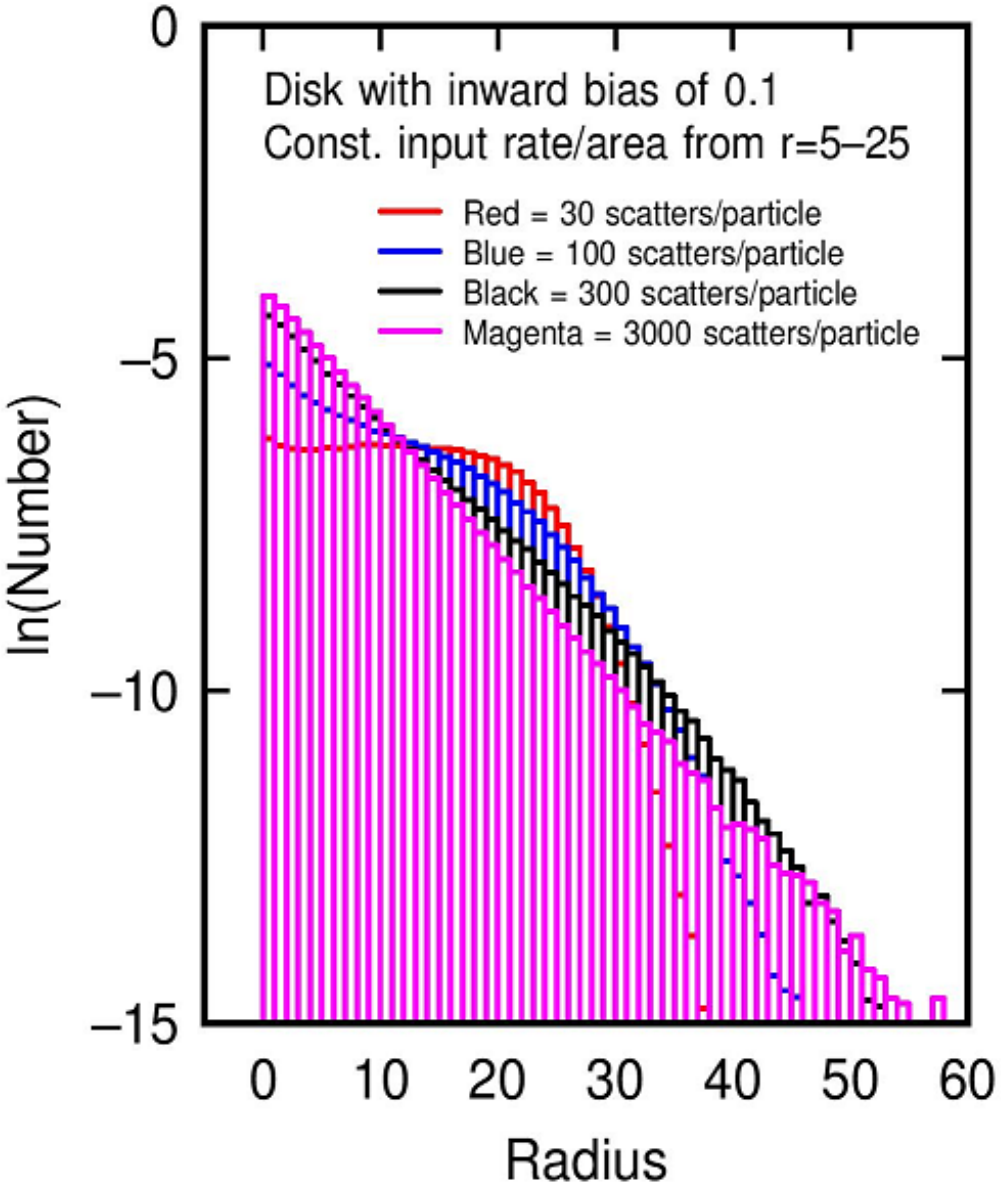
Disk with inward bias of 0.1
Const. input rate/area from r=5–25
Red = 30 scatters/particle
Blue = 100 scatters/particle
Black = 300 scatters/particle
Magenta = 3000 scatters/particle
ln(Number)
0
–5
–10
–15
0
10
20
30
40
50
60
Radius

И даже кусочно-экспоненциальные!

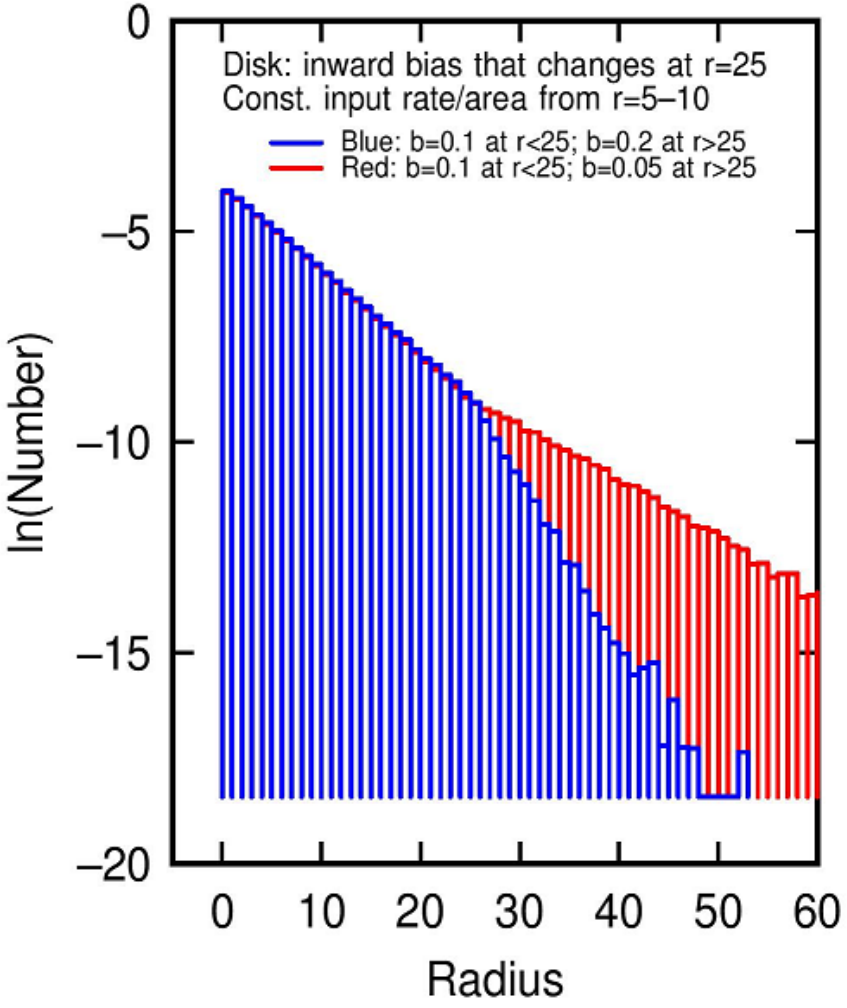

Крумхольц!

2.1 Gravity-Driven Turbulence

To derive the expected relationship between gas content and star formation in a galactic disc where the turbulence is driven by gravity, we consider a system with a flat rotation curve with circular velocity v_c and gas surface density and velocity dispersion versus radius Σ and σ, respectively. The stellar surface density, considering only stars within ~ 1 gas scale height of the midplane, is $\Sigma_* = [(1 - f_g)/f_g]\Sigma$, where f_g is the gas fraction.

For such a setup, Krumholz & Burkert (2010) show that there exists a steady state configuration where turbulence is driven by gravity, ultimately powered by accretion through the disk. The steady state configuration is described by a family of similarity solutions where the gas surface density and velocity disperison versus radius are

$$\Sigma = \frac{v_c}{\pi G Q r}\left(\frac{f_g^2 G\dot{M}}{\eta}\right)^{1/3} \quad (1)$$

$$\sigma = \frac{1}{\sqrt{2}}\left(\frac{G\dot{M}}{\eta f_g}\right)^{1/3}. \quad (2)$$

Крумхольц!

Once Q_g reaches unity and star formation turns on, its rate in these models is determined by the requirement to maintain hydrostatic balance, which implies a star formation rate that varies inversely with the momentum supplied per unit mass of stars formed, and directly as the square of the gas surface density. To be definite we adopt the relation derived by Faucher-Giguère, Quataert & Hopkins (2013, their equation 18), but, as noted in their paper, this result is essentially the same in all feedback-driven turbulence models where Q_g is kept fixed rather than $\epsilon_{\rm ff}$. This relationship is

$$\dot{\Sigma}_* = \frac{2\sqrt{2}\pi G Q_g \phi}{\mathcal{F}} \left(\frac{P_*}{m_*}\right)^{-1} \Sigma^2, \quad (7)$$

where $\phi \approx 1$ and $\mathcal{F} \approx 2$ are constants of order unity that parameterize various uncertainties; the numerical values given here are the ones recommended by Faucher-Giguère, Quataert & Hopkins (2013). The quantity P_*/m_* is the momentum injected per unit mass of stars formed, for which we also adopt Faucher-Giguère, Quataert & Hopkins (2013)'s recommended value of 3000 km s^{-1}. If we now adopt a value the observed weak variation of σ within galaxies, and use equation 6 to eliminate Σ, we can integrate equation 7 with radius to obtain the relationship between star formation rate and gas velocity dispersion,

$$\dot{M}_* = \int_{r_0}^{r_1} 2\pi r \dot{\Sigma}_* \, dr = \frac{8\sqrt{2}\phi v_c^2}{\pi G Q_g \mathcal{F}} \left(\ln \frac{r_1}{r_0}\right) \left(\frac{P_*}{m_*}\right)^{-1} \sigma^2. \quad (8)$$

Comparing equation 5 to equation 8, we see that gravity-driven turbulence models predict $\dot{M}_* \propto f_g^2 \sigma$, while feedback-driven models give $\dot{M}_* \propto \sigma^2$, with no dependence on f_g. In Section 3 we will use these differences to test the models against observations, but first we pause to understand the physical origins of the different scalings, which are two-fold.

Крумхольц: сравнение с наблюдениями

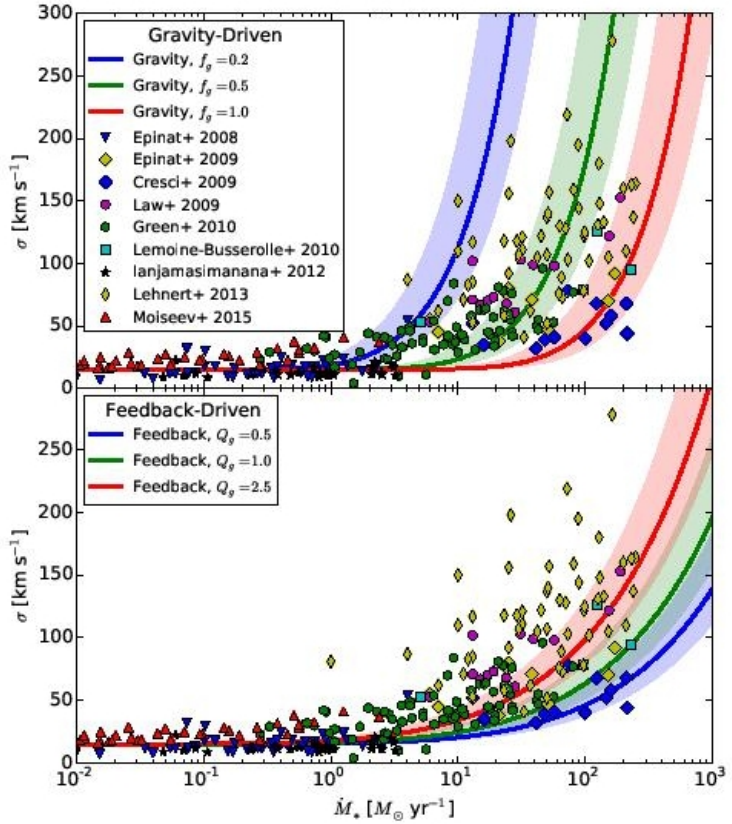

Figure 1. The relationship between star formation rate, $\dot{M}_*$, and velocity dispersion, σ. In the top panel, lines show the predictions of the gravity-driven model (equation 5) for $f_g = 0.2, 0.5$, and 1.0, as indicated in the legend. Lines in the bottom panel show the

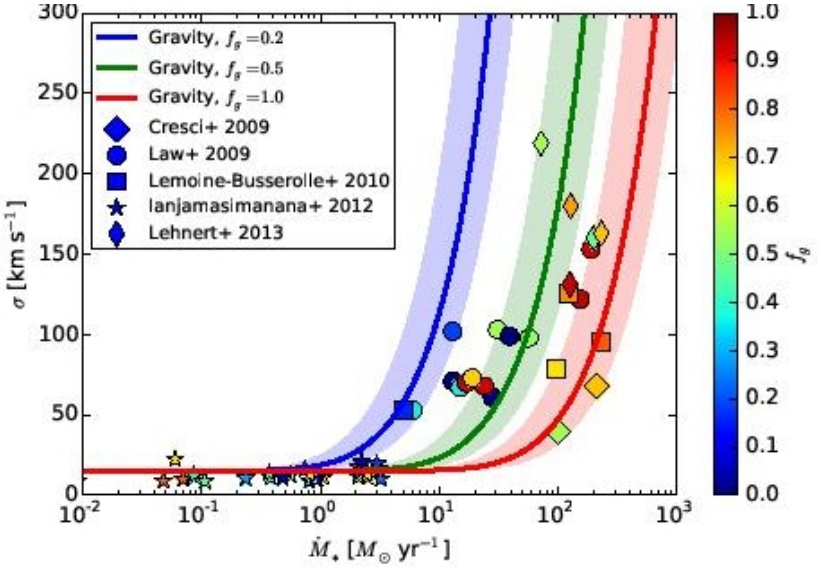

Figure 2. Same as the top panel of Figure 1, but now showing only observations for which a gas fraction is available, and with observed points color-coded by gas fraction, from $f_g \approx 0$ (blue) to $f_g \approx 1$ (red). Data sources are as indicated in the legend, and theoretical models are the same as in the top panel of Figure 1.